Tellus
SERIES B
CHEMICAL
AND PHYSICAL
METEOROLOGY
PUBLISHED BY THE INTERNATIONAL METEOROLOGICAL INSTITUTE IN STOCKHOLM

Tellus (2011), 63B, 831–842
Printed in Singapore. All rights reserved

TELLUS

Five-year analysis of background carbon dioxide and ozone variations during summer seasons at the Mario Zucchelli station (Antarctica)

By P. CRISTOFANELLI[1], F. CALZOLARI[1], U. BONAFÈ[1], C. LANCONELLI[1], A. LUPI[1], M. BUSETTO[1], V. VITALE[1], T. COLOMBO[2] and P. BONASONI[1]*, [1]*National Research Council, Institute of Atmospheric Sciences and Climate Bologna 40129, Italy;* [2]*Centro Nazionale di Climatologia e Meteorologia, Italian Air Force, Pratica di Mare (RM), Italy*

(Manuscript received 19 November 2010; in final form 9 June 2011)

ABSTRACT

The work focuses on the analysis of CO_2 and O_3 surface variations observed during five summer experimental campaigns carried out at the 'Icaro Camp' clean air facility (74.7°S, 164.1°E, 41 m a.s.l.) of the 'Mario Zucchelli' Italian coastal research station. This experimental activity allowed the definition of summer average background O_3 values that ranged from 18.3 ± 4.7 ppbv (summer 2005–2006) to 21.3 ± 4.0 ppbv (summer 2003–2004). Background CO_2 concentrations showed an average growth rate of 2.10 ppmv yr^{-1}, with the highest CO_2 increase between the summer campaigns 2002–2003 and 2001–2002 (+2.85 ppmv yr^{-1}), probably reflecting the influence of the 2002/2003 ENSO event. A comparison with other Antarctic coastal sites suggested that the summer background CO_2 and O_3 at MZS-IC are well representative of the average conditions of the Ross Sea coastal regions. As shown by the analysis of local wind direction and by 3-D back-trajectory calculations, the highest CO_2 and O_3 values were recorded in correspondence to air masses flowing from the interior of the Antarctic continent. These results suggest that air mass transport from the interior of the continent exerts an important influence on air mass composition in Antarctic coastal areas.

1. Introduction

Carbon dioxide (CO_2) and tropospheric ozone (O_3) have major roles in determining the radiative budget of the atmosphere. Although CO_2 is considered the most important anthropogenic greenhouse gas (GHG), O_3 is ranked as the third most powerful GHG since pre-industrial ages and, by influencing the lifetime of other greenhouse gases, it also has an indirect impact on climate (Forster et al., 2007).

Atmospheric CO_2 concentrations are determined by different processes: respiration and photosynthesis by the terrestrial biosphere, emissions from human activities like fossil fuel combustion and land-use change as well as uptakes by oceans (Forster et al., 2007). In the past years, strong efforts have been made to define accurately the role of CO_2 within the biosphere carbon cycle. In particular, since knowledge of the latitudinal CO_2 gradient is a key issue for the validation of global models describing the carbon budget, measurements conducted at high latitudes constitute a fundamental activity. In Antarctica, due to its remoteness from vegetation cover and industrialized regions, CO_2 levels are mostly determined by air mass transport and processes occurring at the ocean surface (e.g. Murayama et al., 1995; Morimoto et al., 2003). However, particularly in the case of the Southern Ocean (i.e. the southernmost waters of the World Ocean, generally taken to be south of 60°S latitude and encircling Antarctica), there remains contrasting evidence concerning regional CO_2 source/sink distributions, especially during the austral summer (Longinelli et al., 2007 and references therein). For these reasons, CO_2 measurements performed in this area can provide useful data for determining the mean annual global concentration increases, as well as year-to-year variability due to large-scale phenomena, like the El Niño Southern Oscillation (ENSO) (Dettinger and Ghil, 1998). In particular, CO_2 measurements on the east coast of Antarctica can provide new information on CO_2 behaviour in the Pacific coastline region, since all the other existing measurement stations are located in the Atlantic or Indian Ocean coastal sectors (WMO, 2010; Fig. 1).

Several processes influence tropospheric O_3 concentrations in Antarctica: long-range air mass transport (e.g. Murayama

*Corresponding author.
e-mail: p.bonasoni@isac.cnr.it
DOI: 10.1111/j.1600-0889.2011.00576.x

Fig. 1. Geographic location of MZS and MZS-IC (red). Map of Antarctica generated using the 'Antarctic Atlas' web interface of the United States Antarctic Resource Center (http://gisdata.usgs.gov/website/antarctic_research_atlas/).

et al., 1992), spring depletion episodes involving reactive halogen atoms (e.g. Wessel et al., 1998; Roscoe et al., 2001; Tarasick and Bottenheim, 2002) and the production of large O_3 amounts in the summer near-surface boundary layer (Davis et al., 2004; Helmig et al., 2008). Several studies have revealed that, during the summer period, the release of NO_x due to the photolysis of NO_3^- in snow pack interstitial air can occur over the Antarctic Plateau (e.g. Davis et al., 2001; Jones et al., 2001), thus promoting a surprisingly active photochemical environment and net photochemical production.

Within the framework of the Italian National Programme of Antarctic Researches (PNRA), continuous measurements of surface CO_2, O_3 and meteorological parameters were performed at the 'Icaro Camp' clean air facility of the 'Mario Zucchelli' station (74.7°S, 164.1°E, 41 m a.s.l., hereinafter MZS-IC) during five experimental summer campaigns. At this measurement site, a preliminary investigation suggested that air mass transport could significantly affect near-surface O_3 concentrations during December (Cristofanelli et al., 2008). In order to better understand the processes determining the typical summer CO_2 and O_3 background concentrations over the east coast of Antarctica, in the present work, concurrent CO_2 and O_3 variations are investigated as a function of local surface meteorology and 'synoptic-scale' 3-D air mass back-trajectories.

2. Measurement site and experiment

The measurement site is located at Terra Nova Bay on the eastern coast of the Ross Sea, at the confluence of the Reeves and Priestly glaciers (Fig. 1). At MZS-IC, scientific activities are carried out only during the austral summer, when a wide set of experimental activities are conducted. Since 2001, five summer experimental campaigns have been held at 'Icaro Camp', the clean air facility located on the coast, which is 2 km south of the main station. More details on the measurement site and the surrounding area can be found in Argentini et al. (1995) and Cristofanelli et al. (2008).

In the MZS-IC laboratory, the gas (O_3 and CO_2) and air intake is 5 m above surface and consists of a 2-m long Pirex stack enclosed in a steel cover fixed to the shelter roof, while air sampling is forced by a turbo blower. The O_3 measurements were performed by a UV photometric analyser Dasibi 1108 PC, and the raw data were stored at 1-min resolution with a standard uncertainty of ±2 ppbv in the range 1–100 ppbv (on 1-min basis). Zero checks were automatically performed every 24 h.

In addition, after each experimental campaign, the O_3 analyser was delivered to the manufacturer for ordinary maintenance and calibration.

The experimental setup for the CO_2 measurement has been described in a previous paper (Calzolari et al. 2002), so only the main characteristics of the sampling systems are reported here. A non-dispersive infrared (NDIR) analyser (Siemens ULTRAMAT 6E) was used for the continuous determination of CO_2 concentrations at MZS-IC. Two working standards (at about 350 and 385 ppmv) were analysed every 8 h to calibrate the measurement system automatically. For the five experimental campaigns, before shipping to Antarctica, the working standard concentrations were determined against the standards deposited at the GAW-WMO Mt Cimone observatory (code: CMN644N0) in Italy, which is operated by the Italian Air Force Meteorological Service. During a Round Robin experiment conducted on October 2002, the mole fractions measured at the CMN observatory were –0.03 ppmv lower than the one measured by the Global Monitoring Division of the National Oceanic and Atmosphere Administration (NOAA/GMD), formerly CMDL, in the concentration range 370–380 ppmv (WMO, 2010). Moreover, during the fourth and fifth experimental campaigns, the MZS-IC working standard was also check against the standards directly provided by the NOAA/GMD every 7 d. The CO_2 data presented in this work are referred against the WMO-X2007 international scales (Conway et al., 2010; WMO, 2010). In order to minimize the risk of external relative humidity variations determining a different partial pressure of CO_2 in the sample of air, and to prevent any water vapour interference in the IR detection, a new dehumidification system based on the Peltier effect was developed at the Institute for Atmospheric Science and Climate – National Research Council of Italy (ISAC-CNR) and has been employed since 2001 (Calzolari et al., 2002). This instrumental setup permitted excellent measurement linearity (<0.5% of full scale), with precision and repeatability within 0.01 ppmv during optimal sampling conditions.

Standard meteorological parameters (air temperature, relative humidity, atmospheric pressure, wind direction and intensity) were continuously observed with 1-min resolution at a height of 5 m above the ground, using an IRDAM-WST7000 integrated meteorological station. For the 2001–2002 campaign only, relative humidity data were not available due to technical problems.

As the power supply is provided by the main 'Mario Zucchelli' station, the only local pollution at MZS-IC could be due to helicopters and snowcats. Therefore, in situ scientific personnel flagged the measurement periods affected by these activities and the corresponding data were rejected.

In order to determine the origin of air masses reaching the sampling site during the campaign periods, 6-d three-dimensional back-trajectories with 1-h time resolution were systematically calculated every 6 h (at 00, 06, 12 and 18 UTC), using the HYSPLIT model (Draxler and Rolph, 2003). Trajectory calculations, with a horizontal resolution of $1^\circ \times 1^\circ$, are based on meteorological field analyses produced by the National Center for Environmental Prediction (NCEP).

3. Background O_3 and CO_2 behaviours at MZS-IC

3.1. Background data selection

In order to retain data representative of the 'well-mixed' background (i.e. not affected by large variability at the short timescale), a specific multistep selection procedure was applied to the CO_2 data, following the approach presented by Cundari et al. (1995), based on the principle of retaining only measurements characterized by low variability. Using the CO_2 results, a background subset was extracted also for surface O_3 data. Over the five measurement campaigns, this selection methodology allowed the retention of 58% of data as representative of background conditions at MZS-IC. As shown by Cristofanelli et al. (2008), MZS-IC can be occasionally affected by emissions from the main base facilities. In particular, fresh pollution can be transported to the measurement site by northerly winds or during light wind conditions. Therefore, with the aim of evaluating the typical CO_2 and O_3 background values at MZS-IC, data recorded with wind velocity of less than 2 m s^{-1} and wind direction from 22.5 to 335.5° were also excluded. This further screening identified 7% of the data set as potentially influenced by local pollution. For the five summer campaigns, the basic CO_2 and O_3 statistical parameters for the background subsets are reported in Table 1.

3.2. Seasonal and diurnal cycle

To illustrate the summer CO_2 and O_3 cycles at MZS-IC, the average 7-d running mean of daily average values were calculated for the background data (Fig. 2). In order to investigate the seasonal CO_2 behaviour, we detrended the CO_2 data in order to remove the secular growth rate (see the following section). In particular, for each summer campaign, the detrended CO_2 was obtained by subtracting the trend component (calculated by linear fitting) to the observed CO_2 concentrations.

A slight pattern was observed for CO_2 concentrations, with mid-January values –0.50 ppmv lower than those observed at the beginning of November. Despite the relatively small number of analysed years, such behaviour agreed well with the typical seasonal minimum characterizing the annual cycle of CO_2 at high-latitudes sites in the Southern Hemisphere (Murayama et al., 1995; Heimann et al., 1998; WMO, 2010).

As reported in Table 1, for the O_3 background subsets, no systematic interannual trend is observed at MZS-IC, with average concentrations ranging from 18.3 ± 4.7 ppbv (summer 2005–2006, mean value ± 1 standard deviation) to 21.3 ± 4.0 ppbv (summer 2003–2004). The O_3 summer pattern shows a decreasing trend (Fig. 2), with maximum values in November

Table 1. Basic statistical parameters for CO_2 and O_3 at MZS-IC during the five summer campaigns

Parameter	Summer	Mean	*SD*	Min	Median	Max	Number of cases
CO_2 (ppmv)	2001–2002	369.38	0.23	368.87	369.39	369.83	844
	2002–2003	372.23	0.26	371.63	372.17	372.95	733
	2003–2004	374.16	0.31	373.23	374.15	378.84	727
	2004–2005	375.61	0.28	374.13	375.65	376.53	1471
	2005–2006	377.77	0.24	377.10	377.77	378.56	881
O_3 (ppbv)	2001–2002	18.5	2.9	11.8	18.2	27.0	828
	2002–2003	20.9	5.0	11.3	20.0	42.3	735
	2003–2004	21.3	4.0	13.2	20.9	36.9	677
	2004–2005	20.7	4.9	10.0	21.0	37.8	1158
	2005–2006	18.3	4.7	10.0	17.2	35.7	855

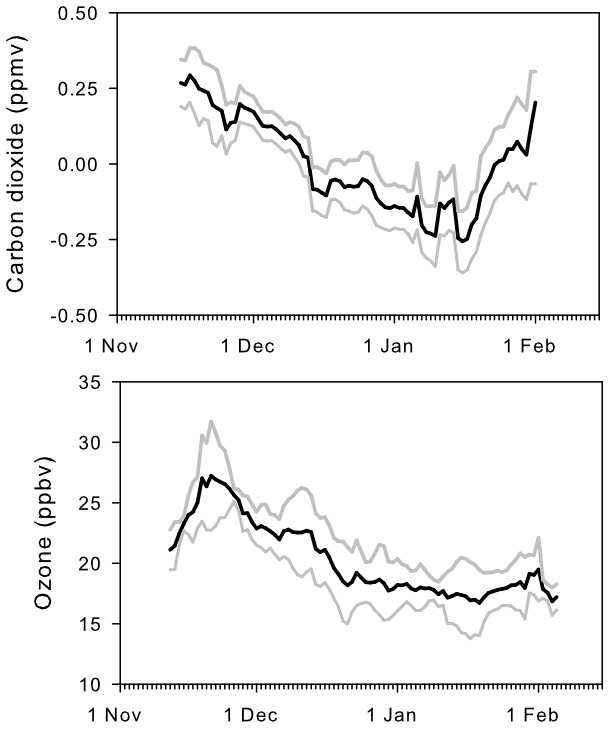

Fig. 2. Calculated average CO_2 (upper panel) and O_3 (lower panel) concentrations at MZS-IC for summer 2001–2005 (black line). The grey lines represent the 95% confidence interval.

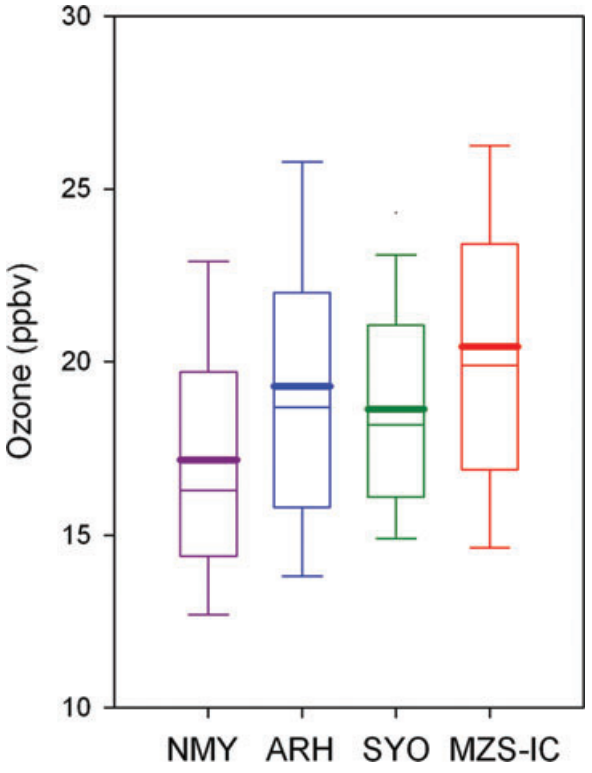

Fig. 3. Comparison of MZS-IC summer O_3 concentrations with simultaneous observations at other Antarctic coastal stations: Neumayer (NMY), Arrival Height (ARH) and Syowa (SYO). The lowest box boundary indicates the 25th percentile, the thin (thick) line inside the box marks the median (mean value) and the highest box boundary indicates the 75th percentile. Whiskers (error bars) above and below the box indicate the 90th and 10th percentiles.

(average monthly mean: 24.5 ± 4.2 ppbv) and the lowest ones in January (18.1 ± 3.3 ppbv). This seasonal minimum is common to other Antarctic coastal sites (Oltmans et al., 2006; Helmig et al., 2007), and is due to the destruction regime dominating over production processes during spring and summer (Crawford et al., 2001; Helmig et al., 2007). The O_3 peak in mid-November results from the episodes of enhanced O_3 concentrations observed during the experimental campaigns. For the same measurement period, a similar feature can be observed also at Arrival Height (ARH; 77°48′S, 166°46′E), located ∼350 km from MZS-IC on Ross Island, near the northeastern edge of the Ross Ice Shelf (here not shown).

For a more detailed characterization of the background O_3 at MZS-IC, O_3 observations at other coastal stations in Antarctica were considered. To this end, daily O_3 values at other stations in Antarctica are shown in Fig. 3, where

the summer background O_3 distribution at MZS-IC is compared with concurring measurements at Neumayer (NMY; 70°39′S, 8°15′W), ARH and Syowa (SYO; 69°00′S, 39°35′ S). In general, the O_3 levels at MZS-IC are very similar (both in average values and variance) with those observed at the other stations. In particular, the average differences range from 3.2 ppbv at NMY to 1.1 ppbv at ARH. The very close agreement with the ARH measurements suggests that the summer background O_3 values at MZS-IC are representative of conditions in the Ross Sea region. As also indicated in Fig. 3, this summer O_3 background is higher than that observed along the eastern Antarctic coastlines, where NMY and SYO are located. Helmig et al. (2007) indicated that O_3 behaviour at ARH is strongly characterized by increase events during November and December, arguing that summer high concentrations at the ARH site could be related to the transport of air masses richer in O_3 from the Antarctic Plateau. Since a similar cause has been suggested by Cristofanelli et al. (2008) to explain the high O_3 values observed in December months at MZS-IC, Sections 3.2 and 4 herein report a specific investigation performed to assess whether air mass transport events could influence trace gas variations at MZS-IC, also providing an estimate of their contributions to the observed CO_2 and O_3 summer variability.

To find out if CO_2 and O_3 background data at MZS-IC were influenced by systematic processes occurring on the 24-h scale (i.e. chemistry or transport processes modulated by solar radiation), the typical diurnal variations of these compounds were calculated in terms of hourly deviations (ΔCO_2 and ΔO_3) from the smoothed seasonal curve, obtained by applying the third-order polynomial fit to the original 1-h data series. On average, no obvious diurnal cycles were evident for CO_2 (Fig. 4). At other Antarctic coastal stations, Helmig et al. (2007) pointed out the existence of small diurnal cycles (higher values in the morning and declining during afternoon–evening) with amplitude of about 0.6–1.5 ppbv, possibly due to O_3 photolysis and chemical destruction by OH and HO_2 during daytime. A small, but still significant (at the 95% confidence level) diurnal variation was observed also for MZS-IC, with a mean amplitude of 0.6 ppbv.

3.3. Interannual CO_2 growth rate

The quasi-steady global increase of CO_2 levels represents one of the main pointers of anthropogenic influence on global atmospheric composition and recent climate changes (Forster et al., 2007). As reported in Table 1, CO_2 observations are characterized by a significant interannual growth rate also at MZS-IC. In particular, in good agreement with the global growth rate observed for the period 2001–2005 (Forster et al., 2007; WMO, 2010), background CO_2 concentrations show an average interannual increase of 2.10 ppmv yr^{-1}, ranging from 369.38 $\pm$ 0.23 ppmv during summer 2001–2002 to 377.77 $\pm$ 0.24 ppmv during summer 2005–2006. The highest growth rate is observed between summer campaign 2001–2002 and 2002–2003 (2.85 ppmv yr^{-1}), probably reflecting the influence of the 2002/2003 ENSO event on the global CO_2 burden (Knorr et al., 2007). To attain a better estimation of the representativeness of MZS-IC observations, the monthly mean CO_2 average at MZS-IC is compared with observations at other Antarctic coastal stations participating to the GAW-WMO programme. Figure 5, for each station (coded by different symbols as reported in the figure legend), reports the four values of monthly average CO_2 from November to February in function of the five experimental campaigns (reported on the *x*-axis as SC-I, SC-II, SC-III, SC-IV and SC-V).

Concerning the five experimental campaigns, the MZS-IC values are in good agreement with data recorded at the other coastal stations of SYO, Halley Bay (HBA; 75°33′S, 26°32′W), Casey (CYA; 66°17′ S, 110°19′E) and Palmer (PSA; 64°55′S,

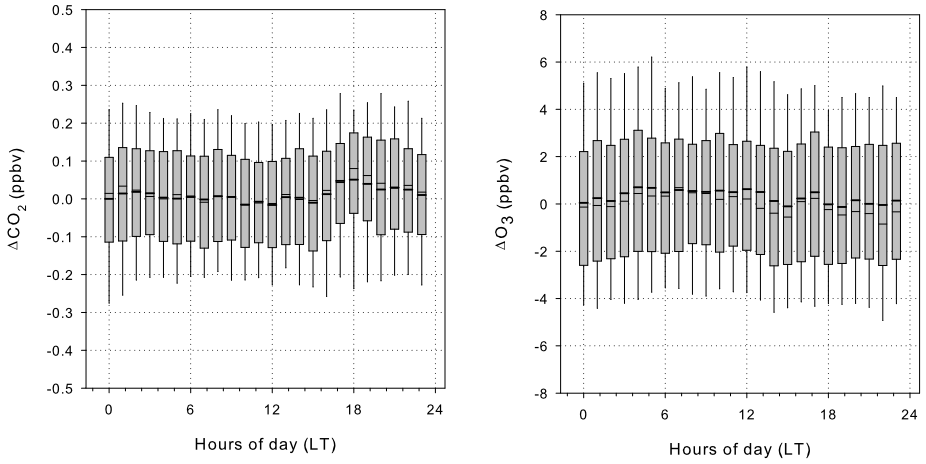

Fig. 4. Diurnal variation of ΔCO_2 and ΔO_3 at MZS-IC. The lower box boundary indicates the 25th percentile, the thin (dashed) line inside the box marks the median (mean value) and the higher box boundary indicates the 75th percentile. Whiskers (error bars) above and below the box indicate the 90th and 10th percentiles.

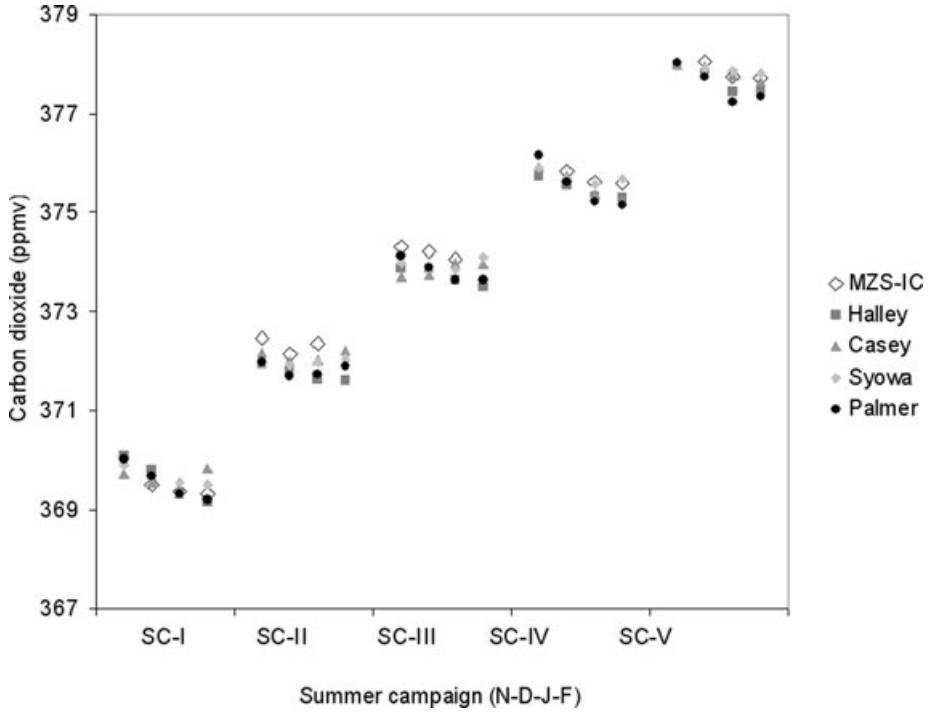

Fig. 5. Monthly average CO_2 values (November, December, January, February) at MZS-IC and other Antarctic coastal stations during the five summer campaigns SC-I (summer 2000–2001), SC-II (summer 2003–2003), SC-III (summer 2003–2004), SC-IV (summer 2004–2005) and SC-V (summer 2005–2006).

64°00′W), there being no evident systematic deviations from these data sets over the five summer seasons: the average summer 2001–2006 growth rate observed at these stations was 2.05 ppmv yr^{-1} (ranging from 2.02 ppmv yr^{-1} at HBA to 2.07 ppmv yr^{-1} at SYO). The highest CO_2 difference is observed at PSA (+0.25 ppm). It can be cautiously argued that this difference might be partially related to the diverse geographical locations of the two stations: in particular, PSA is located more than 10° further north than MZS-IC. In contrast to what is observed over the central Indian Ocean and southern Pacific (Longinelli et al., 2005), this would indicate a (small) increase in CO_2 summer values moving towards higher latitudes in the Southern Hemisphere. Interestingly, the lowest average CO_2 difference was detected in the comparison with SYO (+0.04 ppm). Like MZS-IC, this station is located in a coastal region significantly affected by air masses from the interior of the continent (Suzuki et al., 2004), suggesting that, as detailed in the following section, this type of transport process may be able to advect higher CO_2 concentrations to specific Antarctic coastal areas.

3.4. Background CO_2 and O_3 as a function of local wind regimes and synoptic-scale circulation

To assess the variability of summer background CO_2 and O_3 at MZS-IC, as first step, ΔCO_2 and ΔO_3 were analysed as a function of local wind direction. Table 2 reports the basic statistical parameters of ΔO_3 and ΔCO_2 for each wind sector. Moreover, with the aim of providing an indication of the statistical significance of the results obtained, the expanded uncertainty calculated for the 95% confidence level (coverage factor $K = 2$) is also reported. On average, during the five summer campaigns, the highest values of both compounds were recorded in correspondence to winds blowing from west to northwest sectors (Table 2), which showed significant O_3 and CO_2 increases compared to average values and the remaining wind sectors. As shown by Argentini et al. (1995) and Cristofanelli et al. (2008), air masses reaching MZS-IC from these wind directions can be affected by air masses flowing from the interior of the continent in connection with katabatic winds (Bromwich, 1989). Conversely, as reported in Table 2, the lowest ΔCO_2 and ΔO_3 are observed in correspondence to southerly winds. As shown in the following section, air masses from this wind sector were likely to be advected towards MZS-IC by cyclonic areas over the western Ross Sea (e.g. Davolio and Buzzi, 2002), transporting maritime air masses originating from the external continent belt and ocean boundary layer. This appears to be in agreement with the results of Morimoto et al. (2003) and Legrand et al., (2009), who indicated that during summer CO_2-depleted and O_3-depleted air masses could be transported from lower latitudes to the Antarctic coastlines.

To investigate the influence of synoptic-scale transport patterns on background O_3 and CO_2 variability at MZS-IC,

Table 2. ΔO_3 and ΔCO_2 values as a function of local wind direction at MZS-IC

Parameter	N	NE	E	SE	S	SW	W	NW
ΔO_3 (ppbv)	–	0.42	–0.09	–0.16	–0.78	–0.11	0.85	1.06
	–	*3.38*	*3.05*	*3.45*	*3.45*	*4.22*	*3.74*	*4.50*
	(4)	(716)	(105)	(224)	(853)	(839)	(963)	(510)
	μ : –	μ: 0.25	μ: 0.58	μ: 0.45	μ: 0.23	μ: 0.29	μ: 0.23	μ: 0.29
ΔCO_2 (ppmv)	–0.25	–0.01	–0.04	–0.10	–0.09	0.03	0.03	0.06
	0.27	*0.18*	*0.17*	*0.19*	*0.25*	*0.29*	*0.20*	*0.19*
	(21)	(742)	(108)	(248)	(248)	(957)	(909)	(537)
	μ: 0.11	μ: 0.01	μ: 0.03	μ: 0.02	μ: 0.01	μ: 0.02	μ: 0.01	μ: 0.02

Note: Average mean values, standard deviations (italic), number of data (in brackets) and expanded uncertainty with $p < 0.05$ (μ) are reported.

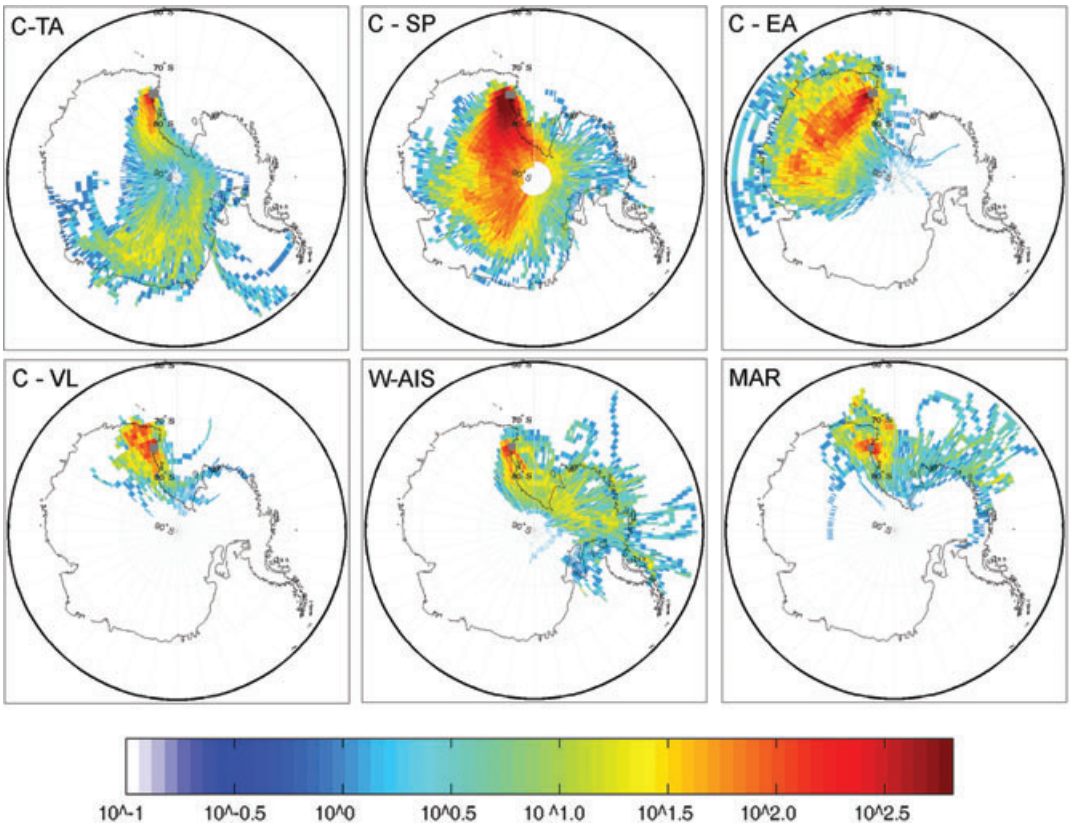

Fig. 6. Air mass clusters arriving at MZS-IC during the five summer 2001–2006 campaigns: C-TA (Continental-Trans Antarctic); C-SP (Continental-South Pole); C-EA (Continental-East Antarctica); C-VL (Continental-Victoria Land); W-AIS (West Antarctica Ice Sheet); MAR (Marine). Colour bar denotes the number of back-trajectories in a $1^\circ \times 1^\circ$ grid domain.

the HYSPLIT back-trajectories were studied using a non-hierarchical cluster analysis (Dorling et al., 1992). A cluster methodology available in the HYSPLIT-tool package was applied: at each step of the agglomeration process, the appropriate number of clusters was determined by analysing the variations of a specific statistical parameter, that is, the total spatial variance (e.g. Tarasova et al., 2007; Dorling et al., 1992). A total of 2137 back-trajectories were analysed during the five summer campaigns and the identified clusters were considered representative for the synoptic-scale circulation affecting MZS-IC during the 6 h centred around the back-trajectory arrival times. The analysis led to the identification of six principal circulation patterns at MZS-IC (Fig. 6):

Table 3. ΔO_3 and ΔCO_2 mean values as a function of air mass back-trajectory clusters

ΔO_3 (ppbv) Cluster	Mean	*SD*	Min	Median	Max	Number of cases	μ	Percentage of occurrences (%)
C-TA	−0.4	3.5	−5.8	−1.4	16.2	320	0.4	9.2
W-AIS	−2.2	2.7	−6.7	−2.7	4.4	173	0.4	5.0
C-SP	0.1	3.5	−10.4	−0.1	14.9	2206	0.1	63.6
C-EA	**2.7**	**3.8**	**−6.9**	**2.7**	**17.5**	**604**	**0.3**	**17.4**
C-VL	−2.0	2.7	−6.9	−2.4	8.4	85	0.6	2.5
MAR	*−3.7*	*2.0*	*−7.4*	*−4.0*	*1.1*	*80*	*0.4*	*2.3*
ΔCO_2 (ppmv)								
C-TA	**0.03**	**0.19**	**−0.63**	**0.04**	**0.62**	**325**	**0.02**	**8.5**
W-AIS	−0.05	0.19	−0.54	−0.03	0.28	203	0.03	5.3
C-SP	−0.01	0.22	−1.23	0.01	3.25	2437	0.01	64.0
C-EA	**0.03**	**0.20**	**−0.61**	**0.04**	**0.66**	**619**	**0.01**	**16.3**
C-VL	−0.10	0.19	−0.81	−0.08	0.24	92	0.04	2.4
MAR	*−0.34*	*0.31*	*−1.40*	*−0.29*	*0.22*	*132*	*0.05*	*3.5*

Note: Highest (lowest) average values are denoted in bold (italic). μ indicates the expanded uncertainty with $p < 0.05$.

(1) Continental-Trans Antarctic (C-TA): air masses that travelled thousands of kilometres across the East Antarctic Ice Sheet, also passing over the Pacific coastlines.

(2) Continental-South Pole (C-SP): air masses that underwent long-range transport, spending a long time over the highest region of the Antarctic Plateau.

(3) Continental-East Antarctica (C-EA): air masses travelling along the Eastern part of the continent and reaching MZS-IC after travelling along the East Antarctica drainage area.

(4) Continental-Victoria Land (C-VL): air masses representative of regional transport, mainly originating over Victoria Land.

(5) West Antarctica Ice Sheet (W-AIS): air masses originating over the West Antarctica Ice Sheet, travelling over the Ross Ice Shelf and Ross Sea before reaching the measurement site.

(6) Marine (MAR): air masses that reached MZS-IC after travelling over the Ross Sea Ice Shelf, which may have interacted with the marine boundary layer over the Ross Sea and Atlantic Ocean.

As reported in Table 3, in good agreement with the ΔCO_2 and ΔO_3 categorization as a function of the local wind regimes, the most frequent air mass circulations were associated with air masses coming from the interior of the continent: C-SP (frequency: 64%) and –C-EA (frequency: 16–17%). Despite its coastal location, considering the synoptic-scale circulation, a relatively small number of air masses were found to be of marine origin at MZS-IC: W-AIS (frequency: 5%) and MAR (frequency: 2–3%). This result is in agreement with the analyses performed by Stohl and Sodemann (2010). Using a Lagrangian particle dispersion model to analyse a 5.5-yr climatology of air mass transport into the Antarctic troposphere, these authors showed that, during summer, the Ross Ice Shelf and East Ross Sea coastlines were characterized by the greatest 'isolation' with respect to air mass transport from middle latitudes.

Concerning CO_2 variations, the highest ΔCO_2 average values (+0.03 ppmv) were observed within continental air masses (C-TA and C-EA). Moreover, a not-negligible fraction (75%) of C-SP air masses were characterized by high CO_2 contents ($\Delta CO_2 > 0.17$ ppmv). According to the analysis of the local wind regime, this means that 6-d-old air masses confined within the interior of the Antarctic continent were also enriched in CO_2 compared to air masses that could have experienced mixing with air masses from lower latitudes or with ocean surfaces (e.g. MAR, W-AIS and C-VL). In particular, the lowest average ΔCO_2 was observed in association with MAR circulation (–0.34 ppmv). This appears to be in good agreement with the earlier work of Murayama et al. (1995), indicating that during summer, low-CO_2 air masses from lower latitudes of the Southern Hemisphere can reach the Antarctic coastlines via low-troposphere transport. An other possible explanation for these low-CO_2 values could be the role played by the Ross Sea and Southern Ocean as CO_2 sinks (Roy et al., 2003). In fact, as derived from the HYSPLIT back-trajectories, a considerable fraction (80%) of MAR air masses was characterized by very low travel altitudes over the sea surface (< 250 m a.g.l.) along their route towards MZS-IC.

The highest average ΔO_3 value (+2.7 ppbv) was observed for the C-EA cluster, indicating that air masses travelling over the eastern continental plateau were significantly enriched in O_3 when arriving at MZS-IC. As shown by the calculated back-trajectories, 60% of C-EA air masses remained below 1 km a.g.l. during the 6-d journey to MZS-IC, suggesting that interaction with the plateau surface was likely. The finding is in agreement with those of Legrand et al. (2009), who evidenced high O_3 val-

Table 4. ΔO_3 and ΔCO_2 (mean values ± expanded uncertainty with $p < 0.05$, with 'N' indicating the number of hourly data) for 'katabatic' events at MZS-IC and remaining periods ('No katabatic')

	All data		November–December		January–February	
Parameter	Katabatic	No katabatic	Katabatic	No katabatic	Katabatic	No katabatic
ΔO_3 (ppbv)	1.1 ± 0.1	–0.9 ± 0.1	1.4 ± 0.2	−1.4 ± 0.2	0.7 ± 0.2	−0.3 ± 0.1
	N: 3186	*N*: 3754	*N*: 2072	*N*: 1774	*N*: 1240	*N*: 1695
ΔCO_2 (ppmv)	0.02 ± 0.01	0.00 ± 0.01	0.02 ± 0.01	0.00 ± 0.01	0.03 ± 0.01	0.00 ± 0.01
	N: 2845	*N*: 2942	*N*: 1819	*N*: 1446	*N*: 1224	*N*: 1420

Note: The same analysis is presented separately for 'November–December' and 'January–February' data sets. All the available data are considered.

ues at the Dumont D'Urville coastal station (66°40′S, 140°01′E, 40 m a.s.l.) in air masses arriving from the East Antarctic plateau during summer periods. Wang et al. (2008) explained that, due to the efficient emissions from the snow pack, the central part of the East Antarctic plateau surface is characterized by the highest NO_x mixing ratios, and that high O_3 photochemical production rates are expected along the transport towards the coastlines. Conversely, the present analysis suggested that lower ΔO_3 was present in air masses that probably interacted with the ocean surface. In fact, MAR air masses presented the lowest average O_3 (ΔO_3: –3.7 ppbv), but W-AIS and C-VL also showed O_3 contents well below the summer average.

4. Influence of katabatic winds on CO_2 and O_3 variations

Terra Nova Bay is one of the Antarctic coastal areas most affected by katabatic surface winds (Bromwich, 1989), being located at the confluence of the Reeves and Priestly glaciers which represent primary routes for katabatic flows in this area (Viola et al., 1999; Davolio and Buzzi, 2002). Even though katabatic wind events are less frequent during summer than winter, synoptic forcing (Bromwich et al., 2003) or diurnal variations of horizontal and vertical temperature gradient (Cava et al., 2004) are able to drive negatively buoyant air from the Antarctic Plateau into the narrow glacial valleys (e.g. Priestly and Reeves glaciers) and, finally, over the steep coastal slopes.

Previous works (Cristofanelli et al., 2008; Helmig et al, 2007; Legrand et al., 2009) have suggested that katabatic flows are likely to affect trace gas variations at Antarctic coastal stations. Thus, due to its topographic characteristics and thanks to the existence of a high-quality Automatic Weather Station (AWS) network, the MZS-IC region is a suitable location for specifically investigating the influence of katabatic flows on summer CO_2 and O_3 variations. With the specific purpose of attaining an accurate evaluation of this issue, an analysis was performed of the wind data recorded at the AWS 'Zoraida' (AWS-Z; 74.25°S, 163.17°E), which is located on the Priestly Glacier (Fig. 1). As indicated by Argentini et al. (1995) and Davolio and Buzzi (2002), strong persistent air mass flows observed at this AWS can be used to flag occurrences of katabatic events at MZS-IC. Considering all the summer campaigns, 49% of days were characterized by more than 12 h with wind speed continuously above 10 m s^{-1} at the AWS. At MZS-IC, such periods were characterized by significantly (at 95% confidence level) lower relative humidity (45 ± 14%) than in the rest of the investigated data set (63 ± 16%). In agreement with Bromwich et al. (2003), this further suggests that drier air masses associated with katabatic downward motion could affect MZS-IC when high wind speeds are observed at AWS-Z. The analysis of the synoptic circulation by HYSPLIT back-trajectories showed that, in the selected periods, the occurrence of C-EA air masses increased to 22.6%, whereas MAR air masses almost disappeared (0.4%). The statistical analysis of the CO_2 and O_3 variations recorded during such events are reported in Table 4. It is important to note that the background selection methodology could lead to the rejection of strong variations related to katabatic event occurrences. For this reason, all data are considered here, regardless of whether they were flagged as background or not.

As compared with the remaining summer periods (Table 4), the analysis led to the conclusion that on average periods with katabatic flows at AWS-Z were characterized by higher O_3 (ΔO_3: +2.0 ppbv), whereas only small variations were recorded for CO_2 (ΔCO_2: +0.02 ppmv). However, during specific katabatic episodes at MZS-IC, O_3 and CO_2 increase episodes of more than 15 ppbv and 1 ppmv were detected, thus suggesting that such transport processes effectively influence trace gas behaviours at MZS-IC. The greatest O_3 increases (averaged ΔO_3: +2.8 ppbv) were systematically recorded during katabatic events observed during the period November–December (Table 4). Jones and Wolff (2003) suggested that high O_3 episodes due to NO_x emissions from the snow pack were more frequent during November–December over the Antarctic Plateau. Thus, the present findings at MZS-IC coastal station could represent indirect evidence of the different O_3 production potential of the lower Antarctic atmosphere during the different summer months. In contrast with what was observed for O_3, only small ΔCO_2 variations were observed during katabatic events

in the January–February period, when an average increase of +0.03 ppmv was recorded.

5. Summary and conclusions

The work presents an analysis of CO_2 and O_3 surface variations observed at Terra Nova Bay (Antarctica) during five summer experimental campaigns. The observations were carried out at the 'Icaro Camp' clean air facility (74.7°S, 164.1°E, 41 m a.s.l.), not far from the Italian 'Mario Zucchelli' station on the eastern Ross Sea coastline. Background CO_2 concentrations showed an average growth rate of 2.10 ppmv yr^{-1}, ranging from 369.28 ± 0.23 ppmv (summer 2001–2002) to 377.77 ± 0.24 ppmv (summer 2005–2006). In agreement with Longinelli et al. (2005), and in good agreement with data recorded at other Antarctic coastal stations, the highest CO_2 growth rate was observed between summer campaign 2001–2002 and 2002–2003 (2.85 ppmv yr^{-1}), probably reflecting the influence of the 2002/2003 ENSO event on the global CO_2 burden (Knorr et al., 2007). Summer average background O_3 values ranged from 18.3 ± 4.7 ppbv (summer 2005–2006) to 21.3 ± 4.0 ppbv (summer 2003–2004). As derived from a comparison with other Antarctic coastal sites, the summer CO_2 and O_3 background at MZS-IC were found to be well representative of the average conditions of the Ross Sea coastal regions. On average, no evident diurnal cycles were observed for CO_2, whereas O_3 was observed to undergo a small average diurnal variation (average amplitude: 0.6 ppbv), with slightly higher values before local noon. Such behaviours suggest that no strong local emissions (natural or anthropogenic) affected CO_2 and O_3 at MZS-IC during the selected 'background' periods.

Both CO_2 and O_3 analysis as a function of local wind direction, and 'synoptic-scale' investigation by means of 3-D air mass back-trajectories, found that the highest values were recorded in correspondence to air masses flowing from the interior of the Antarctic continent. As deduced from the analysis of HYSPLIT 3-D back-trajectories, air masses originating over the continent exceeded by 0.4 ppmv the average CO_2 concentration observed during maritime atmospheric circulation. This can be explained by the fact that air masses coming from lower latitudes in the Southern Hemisphere can be characterized by lower CO_2 levels due to the influence of terrestrial biogenic uptake related to the summer biogenic activity (Morimoto et al., 2003). Moreover, as indicated by previous studies (e.g. Roy et al., 2003), during summer, the Ross Sea and Southern Ocean can represent an effective CO_2 sink.

As suggested by Murayama et al. (1995) and Aoki and Nakazawa (1997), 'CO_2-rich air masses could be transported via upper troposphere from low latitudes and Northern Hemisphere' to Antarctic coastal sites. Thus, the higher CO_2 values observed at MZS-IC in correspondence to air masses from the inner Antarctic continent (C-TA, C-SP, C-EA air masses) could be fed by long-range transport occurring via the upper troposphere. Lagrangian air mass transport analyses like those performed here cannot completely elucidate this kind of processes. In fact, the 6-d air mass back-trajectory analysis suggests only a small direct influence of upper 'free troposphere' air masses on MZS-IC. According to the HYSPLIT analyses, air masses originating at altitudes higher than 2 km a.g.l. were 7% within the C-SP cluster and up to 20% for C-EA and C-TA circulations. Moreover, even extending the timescale of the experiment to 30 d, as already done by Stohl and Sodemann (2010), only a limited influence of direct transport from South America, Africa and Australia can be detected for the Antarctic surface. However, setting similar Lagrangian experiments with longer timescales would introduce excessively large uncertainties to obtain conclusive results (Stohl, 1998). More hints could be provided by GCM analyses. In fact, Heimann et al. (1998) pointed out that terrestrial biogenic processes and fossil fuel emissions occurring up to 30°N can significantly affect the seasonal CO_2 behaviours in Antarctica. Thus, it can be argued that the higher CO_2 levels observed when air masses reach MZS-IC from the inner Antarctic continent can be explained also considering contributions from long-range hemispheric-scale transport (Murayama et al.,1995).

The highest average O_3 value (+2.7 ppbv compared to typical summer values) was observed for air masses travelling over the eastern continental plateau where, during summer, efficient NO_x emissions from the snow pack can cause enhanced photochemical O_3 production (Wang et al., 2008).

Finally, for the purpose of evaluating the effect of katabatic winds on CO_2 and O_3 background concentrations, periods were identified that were characterized by summer katabatic flows along the Priestly glacier, one of the main 'drainage channels' by which katabatic winds reach Terra Nova Bay (Bromwich, 1989; Argentini et al., 1995; Davolio and Buzzi, 2002). A statistical analysis indicated that, compared to the remaining periods, CO_2 and O_3 values increased during such events. In specific events, CO_2 and O_3 increases up to 1 ppmv and 15 ppbv were observed, respectively. Such transport processes can therefore partially explain the average differences in air mass composition (both in terms of CO_2 and O_3) between MZS-IC and simultaneous observations carried out at coastal stations not strongly influenced by air mass transport from the interior of the continent (e.g. NMY in the Weddel Sea sector). Together with similar investigations at other measurement stations (e.g. Legrand et al., 2009; Hara et al., 2008), these results suggest that katabatic wind could be a significant factor influencing the atmospheric composition in specific Antarctic coastal regions.

Acknowledgments

This work was carried out within the project DO_3MECO_2 (number PNRA 2004/2.2) funded by the PNRA. The project SHARE (Stations at High Altitude for Research on the Environment) of EV-K2-CNR also contributed to supporting this publication. The

authors gratefully acknowledge the Meteorological Service of Italian Air Force for making available the CO_2 standards at Mt Cimone, and the NOAA Air Resources Laboratory (ARL) for the provision of the HYSPLIT transport and dispersion model and READY website (http://www.arl.noaa.gov/ready.html) used in the publication. The 'Zoraida' meteorological data were provided by the PNRA 'Osservatorio meteo-climatologico' through its website www.climantartide.it. Finally, the authors gratefully acknowledge all the researchers and Institutions who shared the data used in this publication: Rolph Weller (Alfred Wegner Institute) for providing ozone data from Neumayer station; the Office of Antarctic Observations – Japan Meteorological Agency for providing SYO ozone data; Thomas J. Conway (Global Monitoring Division, NOAA/ESRL) for providing carbon dioxide data at Syowa (Japan National Institute of Polar Research), Palmer (United States Antarctic Program) and Halley (British Antarctic Survey) stations (ftp://ftp.cmdl.noaa.gov/ccg/co2/flask/month/); Paul Steele, Ray Langenfelds and Paul Krummel (Commonwealth Scientific and Industrial Research Organisation) for providing carbon dioxide data from the Casey station (Australian Antarctic Division). Ozone measurements at Arrival Height were provided as part of a cooperative program of the U.S. NOAA Earth System Research Laboratory, Global Monitoring Division, the New Zealand Antarctic program and NIWA Lauder, New Zealand. Finally, the authors are grateful to the two anonymous referees for their valuable comments and revisions.

References

Aoki, S. and Nakazawa, T. 1997. Continuous measurement of atmospheric CO_2 concentration at Syowa station (in Japanese). *Antarct. Rec.* **41**, 161–176.

Argentini, S., Del Buono, P., Della Vedova, A. M. and Mastrantonio, G. 1995. A statistical analysis of wind in Terra Nova Bay, Antarctica, for the austral summers 1988 and 1999. *Atmos. Res.* **39**, 145–256.

Bromwich, D. H. 1989. An extraordinary katabatic wind regime at Terra Nova Bay, Antarctica. *Mon. Wea. Rev.* **117**, 688–695.

Bromwich, H. D., Monaghan, A. J., Powers, J. G., Cassano, J. J., He-Lin, W. and co-authors. 2003. Antarctic mesoscale prediction system (AMPS): a case study from the 2000–01 field season. *Mon. Wea. Rev.* **131**, 412–434.

Calzolari, F., Evangelisti, F., Bonafè, U., Colombo, T., Vitale, V. and co-authors. 2002. CO_2 and O_3 concentration measurements at Terra Nova Bay. In: *Italian Research on Antarctic Atmosphere* (ed M. Colacino). SIF, Bologna, 209–225.

Cava, D., Schipa, S., Tagliazucca, M. and Giostra, U. 2004. Some characteristics of atmospheric boundary layer in an Antarctic coastal region. In: *Italian Research on Antarctic Atmosphere and SCAR Workshop on Oceanography* (ed. Colacino, M.). SIF, Bologna, 185–198.

Conway, T. J., Lang, P. M. and Masarie, K. A. 2010. Atmospheric Carbon Dioxide Dry Air Mole Fractions from the NOAA ESRL Carbon Cycle Cooperative Global Air Sampling Network, 1968-2009, Version: 2010–09-08. Available at: ftp://ftp.cmdl.noaa.gov/ccg/co2/flask/month/. Accessed 12 Oct 2010.

Crawford, J. H., Davis, D. D., Chen, G., Buhr, M., Oltmans, S. and co-authors. 2001. Evidence for photochemical production of ozone at the South Pole surface. *Geophys. Res. Lett.* **28**, 3641–3644.

Cristofanelli, P., Bonasoni, P., Calzolari, F., Bonafè, U., Lanconelli, C. and co-authors. 2008. Analysis of near-surface ozone variations in Terra Nova Bay, Antarctica. *Antarct. Sci.* **20**, 415–421.

Cundari, V., Colombo, T. and Ciattaglia, L. 1995. Thirteen years of atmospheric carbon dioxide measurements at Mt. Cimone station, Italy. *Il Nuovo Cimento Series C* **18**, 33–47.

Davis, D., Nowak, J. B., Chen, G., Buhr, M., Arimoto, R. and co-authors. 2001. Unexpect high levels of NO observed at South Pole. *Geophys. Res. Lett.* **28**, 3625–3628.

Davis, D., Chen, G., Buhr, M., Crawford, J., Lenshow, D. and co-authors. 2004. South Pole NO_x chemistry: an assessment of factors controlling variability and absolute levels. *Atmos. Environ.* **38**, 5375–5388.

Davolio, S. and Buzzi, A. 2002. Mechanisms of Antarctic katabatic currents near Terra Nova Bay. *Tellus* **54A**, 187–204.

Dettinger, M. D. and Ghil, M. 1998. Seasonal and interannual variations of atmospheric CO2 and climate. *Tellus* **50B**, 1–24.

Draxler, R. R. and Rolph, G. D. 2003. HYSPLIT (HYbrid Single-Particle Lagrangian Integrated Trajectory) Model access via NOAA ARL READY Website http://www.arl.noaa.gov/ready/hysplit4.html. NOAA Air Resources Laboratory, Silver Spring.

Dorling, S. R., Davies, T. D. and Pierce, C. E. 1992. Cluster-analysis—a technique for estimating the synoptic meteorological controls on air and precipitation chemistry—method and applications. *Atmos. Environ.* **26**, 2575–2581.

Forster, P., Ramaswamy, V., Artaxo, P., Berntsen, T., Betts, R. and co-authors. 2007. Changes in atmospheric constituents and in radiative forcing. In: *Climate Change 2007: The Physical Science Basis*. Contribution of Working Group I to the Fourth Assessment Report of the Intergovernmental Panel on Climate Change (eds Solomon, S., Qin, D., Manning, M., Chen, Z., Marquis, M. and co-editors). Cambridge University Press, Cambridge, United Kingdom and New York, NY, USA, 129–234.

Hara, K., Osada, K., Yabuki, M., Hayashi, M., Yamanouchi, T. and co-authors. 2008. Measurement of black carbon at Syowa station, Antarctica: seasonal variation, transport processes and pathways. *Atmos. Chem. Phys. Discuss.* **8**, 9883–9929.

Heimann, M., Esser, G., Haxeltine, A., Kaduk, J., Kicklighter, D. W. and co-authors. 1998. Evaluation of terrestrial carbon cycle models trough simulation of the seasonal cycle of atmospheric CO2: first results of a model intercomparison study. *Global Biogeochem. Cycles* **12**, 1–24.

Helmig, D., Oltmans, S. J., Carlson, D., Lamarque, J.-F., Jones, A. and co-authors. 2007. A review of surface ozone in the polar regions. *Atmos. Environ.* **41**, 5138–5161.

Helmig, D., Johnson, B., Oltmans, S. J., Neff, W., Eisele, F. and co-authors. 2008. Elevated ozone in the boundary layer at South Pole. *Atmos. Environ.* **42**, 2788–2803.

Jones, A. E., Weller, R., Anderson, P. S., Jacobi H.-W., Wolff, E. W. and co-authors. 2001. Measurements of NO_x emissions from the Antarctic snowpack. *Geophys. Res. Lett.* **28**, 1499–1502.

Jones, A. E. and Wolff, E. W. 2003. An analysis of the oxidation potential of the South Pole boundary layer and the influence of stratospheric ozone depletion. *J. Geophys. Res.* **108**, D18, 4565, doi:10.1029/2003JD003379.

Knorr, W., Gobron, N., Scholze, M., Kaminski, T., Schnur, R. and co-authors. 2007. Impact of terrestrial biosphere carbon exchanges on the anomalous CO_2 increase in 2002–2003. *Geophys. Res. Lett.* **34**, L09703, doi:10.1029/2006GL029019.

Legrand, M., Preunkert, S., Jourdain, B., Gallée, H., Goutail, F. and co-authors. 2009. Year-round record of surface ozone at coastal (Dumont d'Urville) and inland (Concordia) sites in East Antarctica. *J. Geophys. Res.* **114**, D20306, doi:10.1029/2008JD011667.

Longinelli, A., Lenaz, R., Ori, C. and Selmo, E. 2005. Concentration and $\delta^{13}C$ values of atmospheric CO_2 from oceanic atmosphere trough time: polluted and non-polluted areas. *Tellus* **37B**, 385–390.

Longinelli, A., Giglio, F., Langone, L., Lenaz, R., Ori, C. and co-authors. 2007. Atmospheric CO_2 concentrations and $\delta^{13}C$ values across the Antarctic Circumpolar Current between New Zealand and Antarctica. *Tellus* **59B**, 130–137.

Murayama, S., Nakazawa, T., Tanaka, M., Aoki, S. and Kawaguchi, S. 1992. Variations of tropospheric ozone concentration over Syowa Station, Antarctica. *Tellus* **44B**, 262–272.

Murayama, S., Nakazawa, T., Yamazaki, K., Aoki, S., Makino, Y. and co-authors. 1995. Concentration variations of atmospheric CO_2 over Syowa station, Antarctica and their interpretation. *Tellus* **47B**, 375–390.

Morimoto, S., Nakazawa, T., Aoki, S., Hashida, G. and Yamanouchi, T. 2003. Concentration variations of atmospheric CO_2 observed at Syowa Station, Antarctica from 1984 to 2000. *Tellus* **55B**, 170–177.

Oltmans, S. J., Lefohn, A. S., Harris, J. M., Galbally, I., Scheel, H. E. and co-authors. 2006. Long-term changes in tropospheric ozone. *Atmos. Environ.* **40**, 3156–3173.

Roscoe, H. K., Kreher, K. and Friess, U. 2001. Ozone loss episodes in the free Antarctic troposphere, suggesting a possible climate feedback. *Geophys. Res. Lett.* **28**, 2911–2914.

Roy, T., Rayner, P., Matear, R. and Francey, R. 2003. Southern hemisphere ocean CO_2 uptake: reconciling atmospheric and oceanic estimates. *Tellus* **55B**, 701–710.

Stohl, A. 1998. Computation, accuracy and applications of trajectories—a review and bibliography. *Atmos. Environ.* **32**, 947–966.

Stohl, A., and Sodemann, H. 2010. Characteristics of atmospheric transport into the Antarctic troposphere. *J. Geophys. Res.* **115**, D02305, doi:10.1029/2009JD012536.

Suzuki, K., Yamanouchi, T., Hirasawa, N. and Yasunari, T. 2004. Seasonal variations of air transport in the Antarctic and atmospheric circulation in 1997. *Polar Meteorol. Glaciol.* **18**, 98–113.

Tarasick, D.W. and Bottenheim, J.W. 2002. Surface ozone depletion episodes in the Arctic and Antarctic from historical ozonesonde records. *Atmos. Chem. Phys.* **2**, 197–205.

Tarasova, O. A., Brenninkmeijer, C. A. M., Jockel, P., Zvyagintsev, A. M. and Kuznetsov, G. I. 2007. A climatology of surface ozone in the extra tropics: cluster analysis of observations and model results. *Atmos. Chem. Phys.* **7**, 6099–6117.

Viola, A. P., Petenko, I., Mastrantonio, G., Argentini, S. and Bezverhnii, V. 1999. Diurnal variations of the temperature and their influence on wind regime in a confluence zone of Antarctica. *Meteorol. Atmos. Phys* **70**, 133–140.

Wang, Y., Choi, Y., Zeng, T., Davis, D., Buhr, M. and co-authors. 2008. Assessing the photochemical impact of snow NO_x emissions over Antarctica during ANTCI 2003. *Atmos. Environ.* **42**, 2849–2863.

Wessel, S., Aoki, S., Winkler, P., Weller, R., Hrber, A. and co-authors. 1998. Tropospheric ozone depletion in polar regions—a comparison of observations in the Artic and Antarctic. *Tellus* **50B**, 34–50.

WMO—World Meteorological Organization. 2010. WMO WDCGG Data Summary – WDCGG No. 32. Japan Meteorological Agency in collaboration with WMO.